Available online at www.eccomasproceedia.org
Eccomas Proceedia COMPDYN (2025) 1800-1811

ECCOMAS
Proceedia

COMPDYN 2025
10th ECCOMAS Thematic Conference on
Computational Methods in Structural Dynamics and Earthquake Engineering
M. Papadrakakis, M. Fragiadakis (eds.)
Rhodes Island, Greece, 15-18 June 2025

FULL-PROBABILISTIC SEISMIC RESPONSE OF 3D ISOLATED BRIDGES UNDER SPATIALLY VARIABLE EARTHQUAKE GROUND MOTION

Elena Miceli[1], Guglielmo Amendola[1], Massimiliano De Iuliis[1], Gaetano Alfano[1] and Paolo Castaldo[1]

[1] Politecnico di Torino
Corso Duca degli Abruzzi 24, 10129, Turin, Italy
{elena.miceli, guglielmo.amendola, massimiliano.deiuliis, gaetano.alfano, paolo.castaldo}@polito.it

Abstract

In this study, the spectral-representation method is adopted to generate asynchronous excitations on bridges. A probabilistic seismic analysis is conducted on a retrofitted 5-spans reinforced concrete bridge, utilizing non-linear time history analysis within the Opensees platform and modeling the 3D structure. The response of the bridge is compared under uniform and spatially variable seismic input conditions, and its seismic reliability is assessed using incremental dynamic analysis (IDA) and fragility curves. The results demonstrate that spatial variability of earthquake ground motion consistently amplifies the seismic response of bridges compared to uniform ground motion. These results underscore the importance of considering spatial variability of earthquake ground motion in seismic design to improve the safety and resilience of critical infrastructure.

Keywords: Seismic isolation, FPS bearings, Seismic reliability, Spatial variability of earthquake ground motion (SVEGM), Nonlinear Time History Analysis

ISSN:2623-3347
Peer-review under responsibility of the organizing committee of COMPDYN 2025.
doi: 10.7712/120125.12529.24678

1 INTRODUCTION

Bridges play a crucial role in transportation networks, since they are among the most vulnerable infrastructure components during natural disasters [1]-[3]. Unlike buildings, bridges often span long distances, with their support points separated by significant gaps. This makes the spatial variability of earthquake ground motion (SVEGM) a critical factor in their seismic design, aligning with broader aspects on risk management and resilience in infrastructure systems.

The scientific literature has introduced semi-empirical, empirical and analytical coherency models to account for SVEGM phenomena [4]-[8]. This phenomenon arises from the combination of three effects: loss of statistical correlation, the wave-passage effect and the site-response effect. Given the complexity of these phenomena, a deterministic approach to seismic analysis is impractical, necessitating probabilistic methods to capture the uncertainties involved. One such method is the Random Vibration Analysis (RVA) [9], [10], which is statistically robust within the Performance-Based Earthquake Engineering framework but remains too complex for widespread engineering applications. An alternative approach extends the response spectrum method to incorporate SVEGM by applying the principles of random vibration analysis [11],[12]. However, this method is limited to linear or linearized problems, which are inadequate for bridge assessments. Consequently, while computationally demanding, the use of non-synchronous ground motion simulations in time-history analyses is preferred, as it allows for the consideration of both material and geometrical nonlinearities. These simulations rely on different stochastic process modeling techniques that combine power spectral density (PSD) models with coherency functions [13] and the spectral representation method, being one of the most commonly employed [14],[15].

Building on these methodologies, the scientific community has conducted various sensitivity analyses of structures under multiple support excitations. Specifically, numerous non-linear time-history analyses have been performed to investigate the seismic response of different bridge types and configurations subjected to multiple support excitation [7],[16]-[20]. However, relatively few studies have focused on the seismic response of isolated bridges [21],[22]. Seismic isolation is a well-established strategy for enhancing the seismic performance of bridges, effectively reducing earthquake-induced damage. By incorporating mechanical devices with very low horizontal stiffness, seismic isolation decouples the bridge superstructure from its substructure [23]. Among these devices, the friction pendulum (FP) system has proven particularly effective due to its ability to maintain an isolation period independent from the mass of the deck. Several experimental and numerical studies have been conducted to examine the behavior of FP systems [24]-[31].

This paper investigates the effects of SVEGM on the seismic response of reinforced concrete (RC) bridges equipped with FP isolators by comparing their response under uniform and non-uniform seismic input conditions. A 5-span simply supported bridge located near L'Aquila, Italy, serves as the case study. The seismic input is simulated using the spectral representation method as well as considering a spectrum-compatible power spectral density and a complex coherency function. A comprehensive set of 3D non-linear time-history analyses is conducted using OpenSees software [32], with the FP friction coefficient treated as a random variable following a standard normal distribution. To assess the seismic response of the structure across varying intensity levels, incremental dynamic analyses (IDA) are performed. The response in terms of pier drift index is estimated and further processed to derive seismic fragility curves, considering different damage limit states. The seismic reliability of the bridge piers is then evaluated over a 50-year time frame, based on the seismic hazard curves for L'Aquila.

2 DESCRIPTION OF THE CASE STUDY AND NUMERICAL MODELING

2.1 Characteristics of the case study

The case study focuses on an existing simply supported RC bridge, constructed in 1979 and located in central Italy, near the Marche-Abruzzo regional border. The design peak ground acceleration (PGA) of the location for the life safety limit state is 0.3g, in line with [33].

A representation of the bridge is shown in Figure 1. In detail, the bridge spans a total length of 163 meters, consisting of five simply supported spans, each approximately 32 meters long. The deck, which has a width of 12.5 meters, comprises I-girders beams connected by a 27 cm-thick reinforced concrete slab. The substructure features unreinforced elastomeric bearings measuring 70 × 50 × 2 cm, positioned on each girder, and a pier cap with a hollow rectangular cross-section of 11 meters in width. The four RC piers exhibit varying heights: H_1=9.75 m, H_2=13.4 m, H_3=12.35 m, and H_4=10.22 m. Each pier has a circular cross-section with a diameter of 2.6 meters and a longitudinal reinforcement ratio of 1.6%. The transverse reinforcement consists of hoops spaced at 44 cm, leading to a total transverse steel ratio of 0.055%. At both ends, the bridge is supported by seat-type abutments, each measuring 12 meters in width and 3.5 meters in height, containing five elastomeric bearings placed on the abutment stem wall. Both the piers and abutments are founded on pile systems. Given the bridge's geometrical and mechanical characteristics, along with its lack of seismic detailing and the inadequate confinement provided by the transverse reinforcement, it is assumed that a retrofit intervention has been implemented. In this context, the original elastomeric bearings have been replaced with friction pendulum system (FPS) bearings, maintaining the same number and spacing at both the abutments and pier caps.

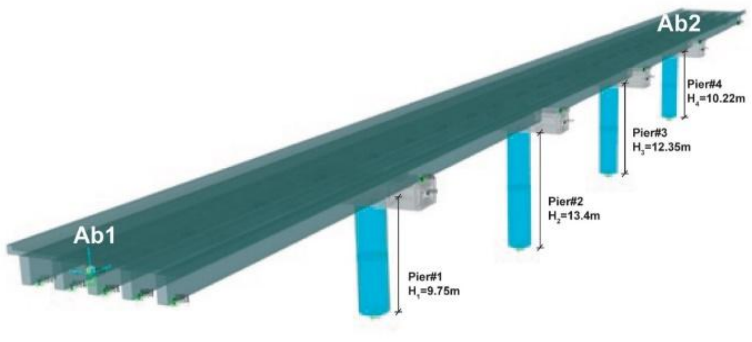

Figure 1: Bridge representation.

2.2 Numerical Modeling

A 3D non-linear finite element (FE) model of the seismically isolated bridge has been developed using OpenSees [32].

The superstructure is assumed to behave elastically under seismic loading. Accordingly, the deck is modeled using five elastic beam-column elements per span, each assigned the appropriate section properties, material characteristics and mass density per unit length.

Material nonlinearity is incorporated exclusively in the RC piers and FPS devices. Each pier is modeled using two Euler-Bernoulli fiber-section, force-based beam-column elements, with a fiber-section approach that includes both confined and unconfined concrete fibers. Geometrical nonlinearity is accounted for by including P-Delta effects in the pier elements. The behavior of the concrete fibers is described using the *Concrete02* material model in OpenSees, which implements the uniaxial Kent-Scott-Park stress-strain relationship [34], that include a stress-strain tensile relationship with a linear tension softening (Figure 2a). The unconfined concrete has a mean compressive strength of 29.1 MPa with a corresponding strain of 2‰, while the confined concrete incorporates an amplification factor of 1.023, as proposed by [35], to account for the effects of confinement. The steel fibers, representing both the longitudinal and transverse reinforcement, follow a uniaxial stress-strain law (*Steel02*), as shown in Figure 2b, with the ultimate strain limited to 0.1 using the *MinMax* material model in OpenSees [32].

The modeling approach for the abutments considers their contribution to the overall bridge stiffness in both the longitudinal and transverse directions. Meanwhile, the isolation system, consisting of five isolators placed at both the pier caps and abutments, is modeled using the *SingleFrictionPendulumBearing* element available in OpenSees [32].

The non-linear system of equations is solved using Opensees, employing the Krylov-Newton iterative algorithm.

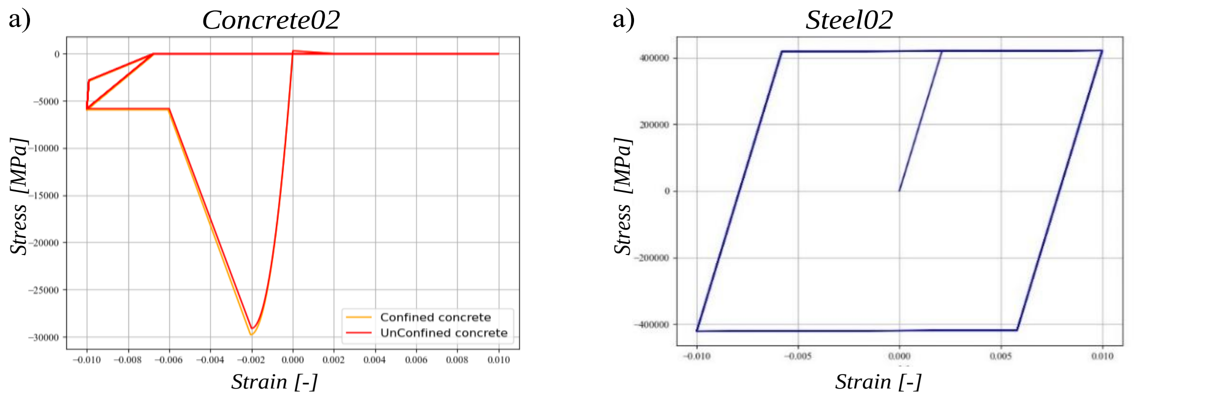

Figure 2: Constitutive laws for the materials of the pier: a) confined and unconfined concrete behavior; b) steel behavior.

2.3 Deterministic and Random Parameters

In this work, different bridge models are obtained by modifying the friction pendulum coefficient.

According to Jangid (2004) [24], the isolation period T_1 and the radius of curvature R are related by the expression: $T_1=2\pi(R/g)^{0.5}$. In this study, an isolation period of 2 sec is considered, corresponding to a radius of curvature of 1 meter.

Furthermore, the effectiveness in dissipating energy [36] of FPS devices is highly dependent on the friction coefficient, which varies with pressure, temperature and sliding velocity. Based on [30],[31], the friction coefficient is modeled as velocity-dependent, following the expression:

$$f = f_{\max} - (f_{\max} - f_{\min})e^{-\alpha|v|} \tag{1}$$

where f_{max} represents the friction coefficient at high sliding velocities, while f_{min} corresponds to its value at low velocities. The parameter α governs the transition between these two states and is set to 30. Following [25]-[29], f_{min} is taken as one-third of f_{max}. Given the uncertainty in the statistical behavior of the friction coefficient under dynamic conditions, f_{max} is treated as a random variable and assumed to follow a standard normal distribution within the range of 2% to 8%. To ensure a representative distribution, ten different realizations of f_{max} are generated using the Latin Hypercube Sampling method.

In accordance with the PBEE principles, the study distinguishes between uncertainties related to seismic intensity variation and those associated with record-to-record variability. To account for randomness in seismic intensity, an intensity measure (IM) is introduced, represented through a hazard curve. Record-to-record variability at a fixed intensity level is addressed by generating a set of scaled seismic records. The chosen IM for this study is the spectral displacement $S_d(\xi_1,T_1)$, corresponding to the isolation period T_1 and damping ratio ξ_1.

A total of 30 artificial acceleration time histories are generated to represent far-field ground motion, under the assumption that the seismic wavefront maintains a constant incidence angle relative to the bridge supports. The selected incidence angle is 60° with respect to the longitudinal axis of the bridge. The seismic input components in the longitudinal and transverse directions are obtained by applying the cosine and sine of the incident angle, respectively, to the generated acceleration time histories following the scaling process.

2.4 Seismic records considering spatial variability

In this work, the method proposed by [37] is adopted to generate fully non-stationary, spectrum-compatible earthquake ground motions. This approach was later extended by [38] for multivariate simulations and is based on the spectral representation method, which enables the generation of a one-dimensional multivariate quasi-stationary stochastic vector process with components $f_k(t)$, where $k=1,\ldots,6$. The index $k=1,\ldots,6$ corresponds to the k-th support point or station in the 5-span. The term quasi-stationary refers to a process where only the amplitude varies with time.

In this study, a set of 30 spectrum-compatible acceleration time histories has been generated at different bridge supports, incorporating a specific coherency model, modulating function, apparent velocity and local site conditions. The simulated time histories are considered partially correlated following the Harichandran and Vanmarcke coherency model [39], which defines the coherency function as:

$$\left|\Gamma_{jk}(\omega)\right| = A\exp\left[-\frac{2\left|\xi_{jk}\right|}{\alpha\theta(\omega)}(1-A-\alpha A)\right]+(1-A)\exp\left[-\frac{2\left|\xi_{jk}\right|}{\alpha\theta(\omega)}(1-A-\alpha A)\right] \tag{2}$$

where the phase spectrum is expressed as:

$$\theta(\omega)=k\left[1+\left(\frac{\omega}{\omega_0}\right)^b\right]^{-0.5} \tag{3}$$

The parameters are set as A = 0.606, a = 0.0222, k = 19,700 m and b = 3.47, based on [39]. The apparent propagation velocity v_{app} along the line connecting stations j and l, separated by a distance ξ_{jl}, , is assumed to be 900 m/s [21].

To account for the non-stationarity of the simulated ground motions, the modulating function proposed by [40] is employed, defined as:

$$A_j(t)=\begin{Bmatrix} \left(\frac{t}{t_1}\right)^2 & t<t_1 \\ 1 & t_1\le t\le t_2=T_s \\ \exp[-\beta(t-t_2)] & t>t_2 \end{Bmatrix} \tag{4}$$

where T_S=t_2-t_1 represents the duration of the stationary phase of the ground motion. The stationary segment is set to 15 seconds.

According to the site classification, the bridge abutments rest on Category A soil (rock), while the piers are supported by Category B soil (very dense sand, gravel, or very stiff clay), as per [33]. Based on this classification, the target elastic response spectra for the site are determined accordingly.

For the simulation of $f_k^{(i)}(t)$, with i=1,…,30, the upper cut-off frequency ω_C is set to 157rad/sec, and the frequency step is defined as $\Delta\omega=\omega_C/N$, being N=1000. The acceleration time histories are simulated over 3000 time steps with a time increment of 0.01 seconds, resulting in a total duration of 30 seconds.

3 INCREMENTAL DYNAMIC ANALYSES

The first step in assessing seismic reliability involves performing Incremental Dynamic Analysis (IDA). This method evaluates the structural response of the bridge under increasing levels of the intensity measure (IM). In this study, the IM is defined as the spectral displacement $S_d(\xi_1,T_1)$, corresponding to the isolation period T_1=2 sec and damping ratio ξ_1=2%.

Following the Italian Guidelines [33], nine different IM levels are considered, corresponding to return periods ranging from 30 to 2475 years. After generating 30 acceleration time histories for each bridge support (i.e., the two abutments and the 5 piers), including the spatially variable earthquake ground motion (SVEGM), each time history is scaled. It is important to note that the scaling is performed before decomposing the wavefront along the transverse and longitudinal directions. A total of 300 non-linear 3D time history analyses is conducted for each of the 9 IM levels. This results from: 1 isolation period, 10 sampled values of the friction coefficients and 30 generated seismic records. Additionally, the results incorporating SVEGM are compared with the same results but assuming uniform excitations. In these cases, the seismic inputs applied at the first abutment (Ab1) of Figure 1 are extended to all bridge supports.

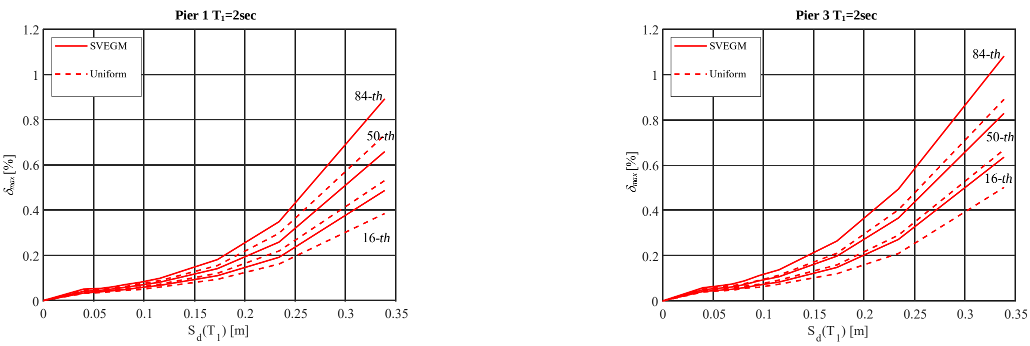

Figure 3: Incremental dynamic analysis results for (left) pier 1 and (right) pier 2.

The primary response parameter or Engineering Demand Parameters (EDP) monitored is the pier drift ratio $\delta(t)$, representative of the relative displacement between the pier top and bottom, normalized by the pier height H. Each response is evaluated as the vectorial sum in the longitudinal and transverse directions over time. To define the EDP, the peak values over time are extracted (i.e., δ_{max}). Hence, for a fixed IM level, a total of 300 EDP values are obtained, combining 30 seismic records with 10 sampled friction coefficients. The EDP is assumed to follow a lognormal distribution [41]-[46], characterized by a geometric mean and dispersion, from which the 16th and 84th percentiles can be calculated [47]-[54].

Figure 3 presents the IDA curves for the maximum vectorial sum of the pier drift ratio δ_{max} comparing the case with asynchronous excitation (i.e., SVGEM) and the case with uniform excitation. For the first left pier (i.e., pier 1), which has a height of 9.75m, the 50th percentile of is slightly lower compared to the third pier, which has a larger height of 12.35m. When increasing the isolation period to 4 seconds, drift ratios are significantly reduced across all piers by more than two-thirds. However, the dispersion of results increases, particularly under SVEGM, which consistently shows greater variability compared to uniform excitation.

4 RELIABILITY ANALYSIS

The seismic reliability assessment follows the PBEE approach. The first step involves determining the seismic fragility, which represents the probability exceeding different damage limit states (LS) at each level of the intensity measure (IM). For the bridge piers, four damage limit states are considered: slight (DLS-1), moderate (DLS-2), extensive (DLS-3), and complete (DLS-4). These LSs, originally developed for non-isolated bridges, are expressed in terms of pier drift ratio using a strain-based criterion. For isolated bridges, the LS thresholds are taken as one-third of those for non-isolated bridges.

The seismic fragility is computed using the total probability theorem, accounting for both cases where the structure does not collapse and where it does. The probability exceeding a given LS threshold is calculated as:

$$P_{LSj}(IM_i = im) = \left(1 - F_{EDP|IM_i=im}\left(LS_{j,EDP}\right)\right)\frac{N_{nc}}{N} + 1\cdot\left(1 - \frac{N_{nc}}{N}\right) \tag{5}$$

where N=300 is the total number of analyses at a fixed IM level, N_{nc} is the number of cases without numerical instability or collapse.

Once the fragility curves are established, the mean annual rate of exceeding a given damage limit state $\lambda_{f,LS}$ is calculated through the convolution integral between the fragility function and the seismic hazard curve λ_S, which describes the mean annual exceedance rate of the intensity measure at the reference site of L'Aquila, Italy. Hence, it applies:

$$\lambda_{f,LS} = \int_s P_{f,LS}[s]\cdot\left|d\lambda_s\right| \tag{6}$$

where $d\lambda_S$ is the derivative of the seismic hazard curve, and $P_{f,LS}[s]$ is the probability exceeding a damage state at a given IM level. Since earthquakes follow a Poisson process, $\lambda_{f,LS}$ is then converted into the probability of exceeding the same damage state within a 50-year time frame using:

$$P_f(50yrs) = 1 - \mathrm{e}^{\lambda_{f,LS}\cdot 50yrs} \tag{7}$$

The computed exceedance probabilities are compared with target failure probabilities ($P_{f,target}$) for different damage states as follows:

- DLS-1: $P_{f,target} = 5\cdot10^{-1}$
- DLS-2: $P_{f,target} = 1.6\cdot10^{-1}$
- DLS-3: $P_{f,target} = 2.2\cdot10^{-2}$
- DLS-4: $P_{f,target} = 1.5\cdot10^{-3}$

These target failure probabilities define the performance objective curve (i.e., PO) while the resolution of Eq. 7 allows to compute the structural performance curve (SP).

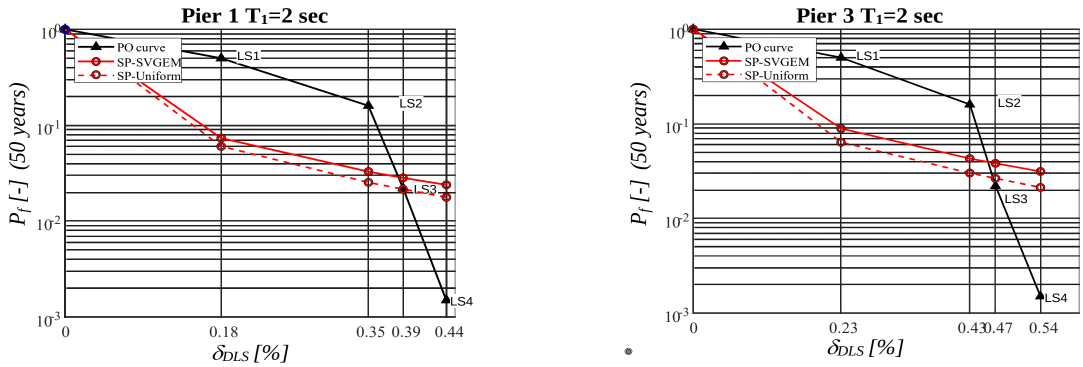

Figure 4: Reliability results for (left) pier 1 and (right) pier 2.

Figure 4 illustrates the exceedance probabilities for the piers over a 50-year period, comparing results for different seismic input models. However, when spatially variable earthquake ground motion (SVEGM) is considered, failure probabilities are consistently higher than in the uniform excitation case, especially for taller piers and at higher damage thresholds.

The fourth damage limit state, associated with a target failure probability of $1.5 \cdot 10^{-3}$, is frequently exceeded across all piers and structural configurations. This is attributed to the stringent threshold adopted for base-isolated bridges.

5 CONCLUSIONS

This study examines the effects of SVEGM on the seismic response of bridges isolated with FP devices. Using the spectral representation method, asynchronous seismic excitations were simulated with a spectrum-compatible power spectral density. A 5-span simply supported RC bridge near L'Aquila (Italy) was analyzed after seismic retrofitting with FP devices, and modeled in OpenSees using a three-dimensional approach that incorporates elastic and non-linear 3D frame elements. Non-linear time history analyses were performed while considering the friction coefficient of the isolators as a random parameter. The seismic response of the bridges under spatially variable input was compared to uniform excitation conditions. By scaling the simulated ground motions to different levels of the selected intensity measure (spectral displacement at the isolation period), IDAs were conducted, focusing on pier drift ratios. The IDA results were then used to derive seismic fragility curves, which were integrated with the seismic hazard curves of L'Aquila to obtain seismic reliability curves. These curves estimate the probability of exceeding specific damage limit states over a 50-year design life. The findings indicate that:

- the inclusion of SVEGM consistently amplifies seismic demands compared to uniform ground motion, particularly at higher intensity measure levels;
- seismic reliability curves reveal that under asynchronous input conditions, the last damage limit state for pier drift is exceeded in most cases. up to 20 cm to satisfy failure probability limits when considering SVEGM.

Further study can investigate the response at the isolation level as well as more bridge configurations and site conditions.

ACKNOWLEDGMENTS

This work was carried out within the RETURN Extended Partnership and received funding from the European Union Next-GenerationEU (National Recovery and Resilience Plan—NRRP, Mission 4, Component 2, Investment 1.3—D.D. 1243 2/8/2022, PE0000005).

This work is part of the research activity developed by the authors within the framework of the “PNRR”: MOST – Sustainable Mobility National Research Center - SPOKE 7 “Cooperative Connected and Automated Mobility and Smart Infrastructures” - WP4" and received funding from the European Union Next-GenerationEU (PIANO NAZIONALE DI RIPRESA E RESILIENZA (PNRR) – MISSIONE 4 COMPONENTE 2, INVESTIMENTO 1.4 – D.D. 1033 17/06/2022).

This work is also part of the collaborative activity developed by the authors within the framework of the WP 15 – Task 15.1 – ReLUIS.

REFERENCES

[1] M. De Iuliis, P. Castaldo, B. Palazzo, Seismic demand analysis of inelastic SDOF systems designed according to the NTC 2008 for L'Aquila earthquake | Analisi della domanda sismica inelastica del terremoto de L'Aquila su sistemi dimensionati secondo le NTC 2008. *Ingegneria Sismica*, **27**(3), 55-68, 2010.

[2] M. De Iuliis, C. Faella, Effectiveness analysis of a semiactive base isolation strategy using information from an early-warning network. *Engineering Structures*, **52**, 518-535, 2013.

[3] L. Petti, M. De Iuliis, Robust design of a single tuned mass damper for controlling torsional response of asymmetric-plan systems. *Journal of Earthquake Engineering*, **13**(1), 108-128, 2009.

[4] A. Zerva, *Spatial variation of seismic ground motions: modeling and engineering applications*. CRC Press, Taylor & Francis Group, 2009.

[5] R.S. Harichandran, A. Hawwari, B. Sweidan, Response of long-span bridges to spatially varying ground motion. *Journal of Structural Engineering, ASCE*, **122**(5), 476-84, 1996.

[6] E. Tzanetos, A. Hamdan, Inelastic dynamic response of RC bridges subjected to spatial non-synchronous earthquake motion. *Advances in Structural Engineering*, **3**, 191-214, 2003.

[7] A. Lupoi, P. Franchin, P.E. Pinto, G. Monti, Seismic design of bridges accounting for spatial variability of ground motion. *Earthquake Engineering and Structural Dynamics*, **34**, 327-48, 2005.

[8] R.S. Harichandran. *Spatial variation of earthquake ground motion: What is it, how do we model it, and what are its engineering applications?*. Michigan State University, 1999.

[9] F. Perotti, Structural response to non-stationary multiple-support random excitation. *Earthquake Engineering and Structural Dynamics*, **19**, 513-27, 1990.

[10] C. Nuti, I. Vanzi, Influence of earthquake spatial variability on differential soil displacements and SDF system response. Earthquake Engineering Structural Dynamics, **34**, 353-74, 2005.

[11] A. Der Kiureghian, A. Neuenhofer, Response spectrum method for multi-support seismic excitations. *Earthquake Engineering Structural Dynamics*, **21**, 713-40, 1992.

[12] A. Der Kiureghian, P. Keshishian, A.M. Halabian, *Multiple support response spectrum analysis of bridges including the site-response effect & the MSRS code*. University of California, Berkeley (CA), 1997.

[13] H. Hao, C.S. Oliveira, J. Penzien, Multiple-station ground motion processing and simulation based on smart-1 array data. *Nuclear Engineering and Design*, **111**, 293-310, 1989.

[14] M. Shinozuka, G. Deodatis, Simulation of stochastic processes by spectral representation. *Applied Mechanics Reviews*, **44,** 191, 1991.

[15] G. Deodatis, Non-stationary stochastic vector processes: seismic ground motion applications. *Probabilistic Engineering Mechanics*, **11**, 149–68, 1996.

[16] A.G. Sextos, K.D. Pitilakis, A.J. Kappos, Inelastic dynamic analysis of RC bridges accounting for spatial variability of ground motion, site effects and soil-structure interaction phenomena. Part 1: methodology and analytical tools. *Earthquake Engineering and Structural Dynamics*, **32**, 607-27, 2003.

[17] A.G. Sextos, A.J. Kappos, Evaluation of seismic response of bridges under asynchronous excitation and comparisons with Eurocode 8-2 provisions. *Bullettin of Earthquake Engineering* **7**, 519-45, 2009.

[18] G. Zanardo, H. Hao, C. Modena, Seismic response of multi-span simply supported bridges to a spatially varying earthquake ground motion. *Earthquake Engineering and Structural Dynamics*, **31**, 1325-45, 2002.

[19] S.P. Papadopoulos, A.G. Sextos, Simplified design of bridges for multiple-support earthquake excitation. *Soil Dynamics and Earthquake Engineering*, **131**, 106013, 2020.

[20] M. Shinozuka, V. Saxena, G. Deodatis. *Effect of spatial variation of ground motion on highway structures*. Princeton (NJ), 2000.

[21] A. Lupoi, The response of isolated bridges accounting for spatial variability of ground motion. *Journal of Earthquake Engineering*, **13**, 814-34, 2009.

[22] S.P. Papadopoulos, A.G. Sextos, Anti-symmetric mode excitation and seismic response of base-isolated bridges under asynchronous input motion. *Soil Dynamics and Earthquake Engineering*, **113**, 148-61, 2018.

[23] I. Buckle, M. Constantinou, M. Dicleli, H. Ghasemi, *Seismic isolation of highway bridges*, 2006.

[24] R.S. Jangid, Seismic response of isolated bridges. *Journal of Bridge Engineering*, **9**(2), 156-166, 2004.

[25] P. Castaldo, G. Amendola, Optimal DCFP bearing properties and seismic performance assessment in nondimensional form for isolated bridges. *Earthquake Engineering and Structural Dynamics*, **50**(9), 2442-2461, 2021.

[26] P. Castaldo, G. Amendola, L. Giordano, E. Miceli, Seismic Reliability Assessment Of Isolated Multi-Span Continuous Deck Bridges. *Ingegneria Sismica*, **39**(3), 26-51, 2022.

[27] P. Castaldo, E. Miceli, Optimal single concave sliding device properties for isolated multi-span continuous deck bridges depending on the ground motion characteristics. *Soil Dynamics and Earthquake Engineering*, **173**, 108128, 2023.

[28] M. De Iuliis, E. Miceli, P. Castaldo, Machine learning modelling of structural re-sponse for different seismic signal characteristics: A parametric analysis. *Applied Soft Computing*, **164**, 112026, 2024.

[29] P. Castaldo, G. Amendola, Optimal sliding friction coefficients for isolated viaducts and bridges. *Structural Control and Health Monitoring*, **28**(12), 2021.

[30] A. Mokha, M.C. Constantinou, A.M. Reinhorn, Teflon bearings in base isolation. I: Testing. *Journal of Structural Engineering*, **116**(2), 438-454, 1990.

[31] M.C. Constantinou, A. Mokha, A.M. Reinhorn, Teflon bearings in base isolation. II: Modeling. *Journal of Structural Engineering*, **116**(2), 455-474, 1990.

[32] F. McKenna, M.H. Scott, G.L. Fenves, Nonlinear Finite-Element Analysis Software Architecture Using Object Composition. *Journal of Computing in Civil Engineering*, **24**(1), 95-107, 2010.

[33] Ministero delle Infrastrutture e dei Trasporti, *DM 17/01/2018 - Aggiornamento delle "Norme Tecniche per le Costruzioni"*, 2018.

[34] D.C. Kent, R. Park, Flexural Members with Confined Concrete. *Journal of the Structural Division - ASCE 97 (ST7)*, 1971.

[35] J.B. Mander, M.J.N. Priestley, R. Park, Theoretical Stress-Strain Model for Confined Concrete. *Journal of Structural Engineering*, **114**(8), 1804-1826, 1988.

[36] M. De Iuliis, E. Miceli, P. Castaldo, An energy framework to control viscoelastic semi-active devices in plan-wise one-way asymmetric systems, *Structural Control and Health Monitoring*, 2025, 10.1155/stc/7091316.

[37] P. Cacciola, A stochastic approach for generating spectrum-compatible fully nonstationary earthquakes. *Computers and Struct*ures, **88**(15-16), 889-901, 2010.

[38] P. Cacciola P, G.A. Deodatis, A method for generating fully non-stationary and spectrum-compatible ground motion vector processes. *Soil Dynamics and Earthquake Engineering,* **31**(3), 351-60, 2011.

[39] R.S. Harichandran, E.H. Vanmarcke, Stochastic variation of earthquake ground motion in space and time. *Journal of Engineering Mechanics*, **112**(2), 154-174, 1986.

[40] P.C. Jennings, G.W. Housner, N.C. Tsai, Simulated earthquake motions for design purpose. *Proceeding of the fourth world conference earth engineering Santiago* **A–1**, 145–60, 1969.

[41] R. Troisi, S. De Simone, M. Franco, Illegal firm behaviour and environmental hazard: The case of waste disposal. *European Management Review*, **21**(3), 605-617, 2024.

[42] R. Troisi, G. Alfano, Is "justice hurried actually justice buried"? An organisational perspective of the Italian criminal justice. *International Journal of Public Sector Management*, **36**(1), 94-109, 2023.

[43] A. Nese, R. Troisi, Individual Preferences and Job Characteristics: An Analysis of Co-operative Credit Banks, *Labour*, **28**(2), 233–249, 2014.

[44] R. Troisi, S. De Simone, M. Franco, The resilience of the regional ecosystems: Healthcare-service organizations, public agents and communities in times of Covid-19. *Mecosan*, (125), 83-97, 2023.

[45] R. Troisi, A. Nese, R. Blanco-Gregory, M.A. Giovanniello, The Effects of Corruption and Innovation on Sustainability: A Firm-Level Analysis. *Sustainability (Switzerland)*, **15**(3), 1848, 2023.

[46] M. Musella, R. Troisi, Property rights and incentives in social cooperatives, *AIEL Series in Labour Economics*, **4**, 47-61, 2009.

[47] E. Miceli, D. Gino, P. Castaldo, Approaches to estimate global safety factors for reliability assessment of RC structures using non-linear numerical analyses. *Engineering Structures*, **311**, 118193, 2024.

[48] D. Gino, E. Miceli, L. Giordano, G.C. Marano, P. Castaldo, Influence of Masonry Infills on Seismic Performance of an Existing RC Building Retrofitted by Means of FPS Devices. *Applied Sciences (Switzerland)*, **13**(6), 3509, 2023.

[49] E. Miceli, S. Ferrara, P. Castaldo, Confinement effects within the seismic design of reinforced concrete frames: reliability assessment and comparison. *Engineering Structures*, **313**, 118248, 2024.

[50] G. Bertagnoli, M. Ferrara, E. Miceli, P. Castaldo, L. Giordano, Safety assessment of an existing bridge deck subject to different damage scenarios through the global safety format ECOV. *Engineering Structures*, **306**, 117859, 2024.

[51] D. Gino, E. Miceli, P. Castaldo, A. Recupero, G. Mancini, Strain-based method for assessment of global resistance safety factors for NLNAs of reinforced concrete structures. *Engineering Structures*, **304**, 117625, 2024.

[52] E. Miceli, P. Castaldo, Robustness improvements for 2D reinforced concrete moment resisting frames: Parametric study by means of NLFE analyses. *Structural Concrete*, **25**(1), 9-31, 2024.

[53] E. Miceli, D. Gino, P. Castaldo, Reliability Assessment Of Robustness For Reinforced Concrete Moment Resisting Frames, Developments in the Built Environment, 2025, 100639, https://doi.org/10.1016/j.dibe.2025.100639.

[54] M. Ferrara, D. Gino, E. Miceli, L. Giordano, M. Malavisi, G. Bertagnoli, Safety assessment of existing prestressed reinforced concrete bridge decks through different approaches, *Structural Concrete*, **25**(3), 1637-1657, 2024.